

SELF-ABSORBED ACTIVE GALACTIC NUCLEI AND THE COSMIC X-RAY BACKGROUND

PIERO MADAU

Space Telescope Science Institute, 3700 San Martin Drive, Baltimore, MD 21218

GABRIELE GHISELLINI

Osservatorio Astronomico di Torino, Strada Osservatorio 20, I-10025 Pino Torinese, Italy

AND

A. C. FABIAN

Institute of Astronomy, Madingley Road, Cambridge CB3 0HA, UK

Received 1993 February 19; accepted 1993 March 24

ABSTRACT

The hard X-ray properties of heavily obscured active galactic nuclei (AGNs) are investigated. We consider the reprocessing of X-rays by photoelectric absorption and Compton downscattering in cold material, and compute the transmitted spectra expected for active galaxies. We discuss the recent OSSE observations in terms of the unified Seyfert scheme, and show that a population of heavily self-absorbed AGNs with an exponential cutoff at high energies may plausibly explain the cosmic X-ray background.

Subject headings: diffuse radiation — galaxies: Seyfert — quasars: general — X-rays: galaxies

1. INTRODUCTION

Thirty years after its discovery by Giacconi et al. (1962), the origin of the cosmic X-ray background (XRB) remains a puzzle. Its spectral shape distinguishes it from every known population of X-ray emitting AGNs: the prime candidates, Seyfert (Sey) galaxies and QSOs, have power-law spectra in the 2–10 keV band which are markedly different from the XRB. Observations from the *Ginga* satellite (Pounds et al. 1990; Matsuoka et al. 1990) have revealed the presence of a flat component in the hard (>10 keV) X-ray spectra of Sey 1 galaxies, along with an iron K-fluorescent line. These findings are generally explained by a “reflection” model in which an incident power law is reflected toward the observer by cold gas, and have soon led to the suggestion that a new population of “reprocessed” AGNs may be at the origin of the XRB. The background energy distribution can be fitted by enhancing the reflected Compton hump relative to the direct power-law component, and by redshifting it to match the XRB peak at 30 keV (Fabian et al. 1990; Rogers & Field 1991; Terasawa 1991; but see Zdziarski et al. 1993). The main problem with this model is the large enhancement required for the reflection component.

Others (Setti & Woltjer 1989; Morisawa et al. 1990; Grindlay & Luke 1990) have suggested an alternative scenario, based on the Sey 1–2 optical unification scheme introduced by Antonucci & Miller (1985). Here, a thick ($N_H \gtrsim 10^{24}$ cm $^{-2}$) molecular torus occults the majority of solid angle around Seyfert nuclei, from the far infrared up to 20 keV. The covering factor of the obscuring torus, as inferred from optical studies, is large: the unfavourably oriented, heavily absorbed Sey 2 galaxies outnumber Sey 1, and therefore contribute substantially to the XRB (Awaki 1991). The obscuration hypothesis is supported by *Ginga* studies of Sey 2 galaxies. The direct X-ray continuum in the prototypical NGC 1068 is hidden from our view by a hydrogen column greater than 10^{25} cm $^{-2}$ (Koyama et al. 1989). The blocking action of thick ($N_H \gtrsim 10^{23}$ cm $^{-2}$) material is also apparent in a large sample of type 2 nuclei (Koyama 1992, p. 74); some are not detected at all. Heavy photoelectric absorption is also present in the UV-detected sample of Mulchaey, Mushotzky, & Weaver (1992), who have

suggested that the nondetection of the optically selected, classical Sey 2 in hard X-rays may be an indication of extremely large columns, like in NGC 1068. Note that to match the turn-over observed in the XRB at high energies, the intrinsic source spectra must steepen beyond a typical energy of ~ 50 keV, as observed in NGC 4151 (Jourdain et al. 1992). This appears to be consistent with the recent observations of Sey 1 galaxies by the OSSE instrument on the *Compton Gamma-Ray Observatory* (Cameron et al. 1993).

We have two purposes in this *Letter*. First, we investigate the hard X-ray properties of obscured AGNs as predicted by the popular unification schemes. In § 2 we consider the reprocessing of X-rays by photoelectric absorption and Compton scattering in cold, Thomson thick material, and compute the transmitted spectra expected for AGNs. We discuss the recent OSSE findings and show that the combination of absorption at low energies, and downscattering together with an intrinsic cutoff in the primary photon distribution at high energies, generates a transmitted spectrum which exhibits a narrow peak in the hard X-ray band. Second, we assess the merits of “reprocessed” AGNs as the root cause of the XRB. In § 3 we study the parameter space available to a simple “obscuration” model and argue that the integrated contribution from self-absorbed Sey 2 can provide a good fit to the XRB only if the obscuring material has Thompson depth $\tau_T \gtrsim 1$ and a large covering factor. A weak cosmic evolution of the candidate sources up to large redshifts is also indicated. We summarize the strengths and weaknesses of this scenario in § 4.

2. X-RAY PROPERTIES OF SELF-ABSORBED ACTIVE GALACTIC NUCLEI

2.1. Transmitted Power-Law Spectra

We approximate the complex geometry of the thick torus which covers the active nucleus of Sey galaxies (see, e.g., Krolik & Begelman 1988) by considering a homogeneous spherical cloud of cold material, surrounding a central source of X-ray photons. We use a Monte Carlo code constructed using the photon-escape weighting method of Pozdnyakov, Sobol', & Sunyaev (1983). The full Klein-Nishina scattering cross section

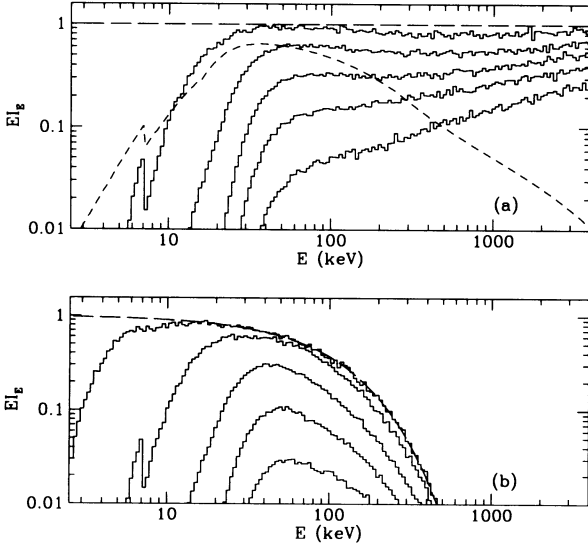


FIG. 1.—Monte Carlo calculations of photon spectra transmitted through a spherical cold cloud of cosmic abundances: the radiation source is at the center. The electron temperature T_e is set to zero, and Compton upscattering consequently neglected. The effects of Compton downscattering and photoelectric absorption have been included. (a) Long-dashed line is the incident spectrum, a power law ($I_E \propto E^{-\alpha}$) with spectral index $\alpha = 1$. The histograms are the transmitted spectra for $\tau_T = 1, 3, 5, 7,$ and 10 ($\tau_* = 1$ at $E_* \simeq 14, 27, 41, 54,$ and 73 keV, respectively). The short-dashed curve is the reflected spectrum from a semi-infinite slab. (b) Incident spectrum is of the form $I_E \propto E^{-\alpha} \exp(-E/kT)$, with $\alpha = 1$ and $kT = 100$ keV (long-dashed line). The histograms are the transmitted spectra for $\tau_T = 0.1, 1, 3, 5,$ and 7 .

is adopted, and the bound-free opacity associated with standard cosmic abundance material is taken from Morrison & McCammon (1983). The results of some Monte Carlo calculations are shown in Figure 1a, where an injected power-law with $\alpha = 1$ is seen in transmission through a cloud which is Thomson thick. The emergent flux is exponentially dimmed below the energy of unity effective absorption depth $\tau_* \simeq [\tau_{\text{abs}}(\tau_{\text{abs}} + \tau_T)]^{1/2}$, with elastic scattering enhancing the photoelectric absorption probability (Rybicki & Lightman 1979). The downscattering of X-ray photons by the cold electrons modifies the transmitted spectrum above the energy $E \sim m_e c^2 / \tau_T^2$ (see, e.g., Sunyaev & Titarchuk 1980): only $\sim 70\%$ (40%) of the power incident in the range 50–400 keV directly escapes from such a medium with $\tau_T = 3$ ($\tau_T = 5$). This percentage progressively increases in the γ -ray region due to the Klein-Nishina reduction of the Compton cross section at high energies. For comparison, Figure 1a also depicts the Compton reflected hump associated with the same incident spectral distribution. The primary photons now originate externally to a semi-infinite, plane-parallel, cold slab (Lightman & White 1988). Hard X-ray photons are forward scattered deep in the medium, degraded in energy, and thus few of them can reemerge before being absorbed. The semi-infinite slab approximation is adequate provided the reflecting material has depth $\tau_T > 10$.

2.2. OSSE Observations of Active Galaxies

Until recently, there were insufficient spectra of AGNs measured at high energies to provide stringent constraints on their contribution to the hard X-ray background. The OSSE instrument on board of the *Compton Observatory* has now observed continuum emission from nine Sey 1 galaxies at photon energies $\gtrsim 60$ keV (Cameron et al. 1993), with a detection rate close

to 100%. The measured γ -ray spectra are very soft, compatible with steep power laws or with thermal emission models with temperatures around 60–100 keV (as in NGC 4151, Maisack et al. 1993). Only one narrow-line AGN (the nearby radio galaxy Cen A) has been detected, and upper limits for 2 Sey 2 galaxies (NGC 1068 and NGC 4593) have been reported. Here, we wish to remark that the OSSE data can test the unified Seyfert scheme and provide an estimate of the absorbing column. Let us assume that Seyfert galaxies are characterized by a primary X-ray spectrum of the form $I_E \propto E^{-\alpha} \exp(-E/kT)$. After being reprocessed by cold material along the line of sight, the emergent intensity per logarithmic energy interval forms a hump, whose position and width are determined by the competition between bound-free absorption at low energies, and Compton down scattering and exponential roll-off of the injected spectrum at high energies. As a result, the entire emergent spectrum is reduced when $\tau_T > 1$, as shown by Figure 1b. If the unified scheme is correct, and the blocking torus is Thomson thick, then the obscured Sey 2 galaxies (at low z) must be much fainter (virtually undetectable if $\tau_T \gg 1$) than Sey 1 at all X-ray frequencies less than 30 keV. The reported OSSE upper limits for Sey 2 might support this model. The alternative scenario, in which OSSE might have detected the Compton turnover of a reflected component appears to require an anomalously large covering fraction of the cold reflecting material, which seems inconsistent with *Ginga* observations of Sey galaxies.

3. AN OBSCURATION MODEL FOR THE X-RAY BACKGROUND

3.1. Comparison with the Data

The XRB is characterized by a peak in $E I_E$ (or, equivalently, a break in the specific intensity I_E) at $E_p \simeq 30$ keV; the lower and upper half-maximum energies are at $E_l \simeq 5$ keV and $E_u \simeq 90$ keV, respectively. The soft X-ray background (SXR) below 3 keV appears as a distinct, steeper component (Wu et al. 1990; Hasinger et al. 1991). About 40% of this soft excess is resolved at 1 keV by *ROSAT* (Shanks et al. 1991; Hasinger 1992) into point sources with $\alpha \sim 1$ –1.2. After subtracting out this soft component, the residual background is very flat, $\alpha \sim 0$, in the 10–20 keV range (as estimated by Giacconi & Zamorani 1987), and is actually inverted ($\alpha < 0$) in the 3–6 keV range, the likely signature of the onset of photoelectric absorption in the sources responsible for the XRB.

For simplicity, and to limit the number of free parameters, we neglect Compton reflections in the following,¹ and assume that the observed background is made up by unresolved, heavily self-absorbed AGNs with primary spectra of the form given in § 2.2. The spectral shape of the XRB severely constrains the parameter space of the obscuration model (see Zdziarski et al. 1993 for a similar discussion about the reflection model). In particular, the individual sources responsible for the background must peak (in $E I_E$) at $E_p \gtrsim 30$ keV, with $E_u/E_p \lesssim 3$; these constraints become even more severe if the XRB results from the sum of contributions over a wide redshift range since any integration in z tends to broaden the resulting spectrum and decrease the observed peak energy. In Figure 2 we show the energy E_p and the ratio E_u/E_p derived for an individual source at $z = 0$, as a function of τ_T , for different

¹ The possible reprocessing of the primary spectrum by reflections will only affect weakly our results provided the covering factor of the cold gas at the X-ray source is $\lesssim 0.5$. Compton reflection models with partial covering are discussed by Terasawa (1991).

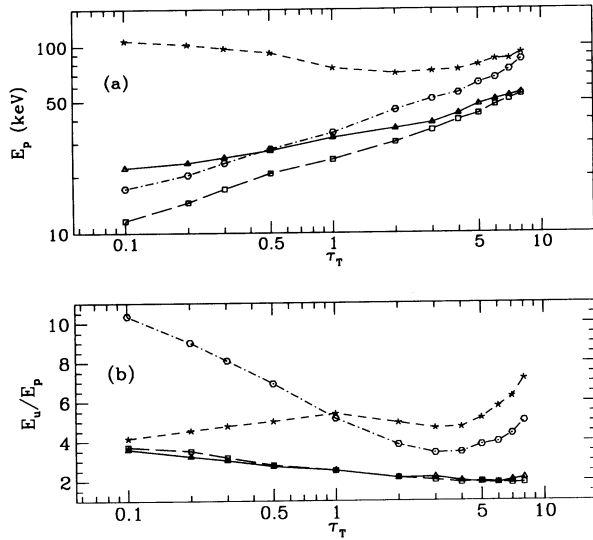


FIG. 2.—Peak energy E_p (a) and the ratio E_u/E_p (b) measuring the width of the transmitted spectrum, plotted as functions of τ_T for $\alpha = 0.7, 1$ and $kT = 50, 360$ keV. All models have been calculated assuming an incident spectrum of the form $I_E \propto E^{-\alpha} \exp(-E/kT)$. Squares: $\alpha = 0.7$, $kT = 360$ keV; circles: $\alpha = 0.7$, $kT = 50$ keV; stars: $\alpha = 1$, $kT = 360$ keV; triangles: $\alpha = 1$, $kT = 50$ keV. The observations require $E_p > 30$ keV and $E_u/E_p < 3$.

values of α and kT . When $\tau_T \ll 1$ and $\alpha < 1$, the position of the peak is completely determined by the exponential roll-off of the primary spectrum, $E_p = (1 - \alpha)kT$, and is independent of τ_T . Downscattering of hard photons in the exponential tail starts to modify the transmitted flux for $\tau_T > 0.1$ and, when $\tau_T \gtrsim 1$, Compton recoil effects dominate at all energies. The width of the hump has its minimum for values of τ_T around a few. Note that the observations require $50 \lesssim kT \lesssim 400$ keV for any value of α . We conclude that the region in the (E, τ_T) plane corresponding to $\tau_T < 1$ is not allowed, as we cannot accurately fit both the position and the (rather narrow) width of the XRB peak for any value of kT and $\alpha \gtrsim 0.7$. Therefore, if self-absorbed AGNs significantly contribute to the XRB, they must be thick to Thomson scattering.

3.2. A Seyfert 2-Dominated XRB

The integrated emission from partially covered, flat X-ray spectrum Sey galaxies can provide a good fit to the XRB in the 3–100 keV range. Figure 3 shows a comparison between the data and a model with $\alpha = 0.7$, $kT = 150$ keV, and $\tau_T = 2.5$

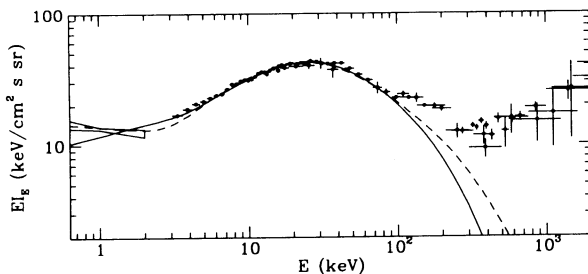


FIG. 3.—XRB produced by partially covered Seyfert galaxies, compared with the data. An empirical fit to the *ROSAT* SXRB spectrum (shown by the elongated 0.5–2 keV error contour) gives $I_E \simeq 13.4 E^{-1.1}$ keV cm $^{-2}$ s $^{-1}$ sr $^{-1}$ keV $^{-1}$. The extrapolation of the $E^{-1.1}$ power law to higher energies provides $\sim 20\%$ of the total XRB intensity at 30 keV. Solid line: flat-spectrum $\alpha = 0.7$ case. Short-dashed line: steep-spectrum $\alpha = 1.1$ case. See § 3.2 for the model parameters.

(solid line). Only a fraction, $f = 0.35$, of the primary radiation is directly observed, while $1 - f$ is reprocessed by the cold material. In the unified scheme $f/(1 - f)$ represents the number ratio of type 1 to type 2 Seyferts. Type 2 objects are the dominant contributors at all energies greater than 3 keV. The comoving bolometric volume emissivity is assumed to evolve as $\langle nL \rangle \propto (1 + z)^C$, with $C = 2.2$ in an Einstein–de Sitter cosmology, up to $z_{\max} = 5$. The model normalization yields for the 2–10 keV emissivity at $z = 0$ (which is completely dominated by type 1 objects), $\langle nL \rangle_{2-10}^0 \simeq 5 \times 10^{38} h_{50} \text{ ergs s}^{-1} \text{ Mpc}^{-3}$ ($h_{50} \equiv H_0/50 \text{ km s}^{-1} \text{ Mpc}^{-1}$), comparable to the 2–10 keV AGN emissivity at the present epoch derived from the Piccinotti et al. (1982) luminosity function. The value of the evolutionary parameter C is consistent with that derived for X-ray selected AGNs from the *Einstein* EMSS sample (Della Ceca et al. 1992), and is smaller than that characteristic of optically selected QSOs (Boyle 1991). Values of $C > 2.5$ are excluded, as they would shift the XRB peak to $E_p < 30$ keV. We remark that this model does not address the intensity of the *ROSAT* SXRB and, as it stands, of the hard XRB above 100 keV.

Note that this population of heavily absorbed Sey 2 galaxies would not have contributed significantly to surveys at the sensitivity of either *HEAO 1* or *Ginga* in the 2–10 keV band. X-ray source counts predicted on the basis of the above model show that the dominant contributors to the energy density of the XRB do not become detectable in the 2–10 keV band until fluxes lower than a few 10^{-13} ergs cm $^{-2}$ s $^{-1}$ are reached. Below that flux we expect the objects to contribute at the level of about 10% of the extrapolated Piccinotti et al. (1982) source counts. Such heavily absorbed Sey 2 should be detectable with *ASCA*. They could be detectable at higher fluxes in the 2–10 keV band if some of the radiation is scattered into our line of sight, as appears to be the case for NGC 1068 and perhaps NGC 4945 (and could also be the case for some of the other X-ray detections of Sey 2). A single population of partially covered steep X-ray spectrum AGNs could actually fit the entire XRB from 0.5 to 100 keV. The dashed curve in Figure 3 depicts a comparison between the data and our best model with $\alpha = 1.1$, $kT = 360$ keV, $\tau_T = 2.5$, $f = 0.12$, $C = 2.2$, $z_{\max} = 7$, and $\langle nL \rangle_{2-10}^0 \simeq 4 \times 10^{38} h_{50} \text{ ergs s}^{-1} \text{ Mpc}^{-3}$. A larger cutoff energy kT is required with increasing α , because of more soft photons and fewer hard photons in the incident spectrum.

It is important to stress that we have not attempted to “best-fit” the model parameters. Also, the obtained large values of z_{\max} should be considered as only indicative, as they are required to accurately fit the observed background flux in the 3–20 keV range, with the bulk of the contribution at energies $E \gtrsim 30$ keV coming from sources at intermediate redshifts, $z \sim 2-3$. A lower z_{\max} could then be more realistic if a significant fraction of the 3–20 keV intensity is due to other sources (e.g., starburst galaxies), or if there is a sizeable dispersion in the properties of individual AGNs, which will tend to broaden the computed XRB hump.

4. CONCLUSIONS

Several arguments suggest that the XRB cannot have either rare, bright QSOs or low- z AGNs as major contributors (for a review see Fabian & Barcons 1992). We know that the residual SXRB at ~ 1 keV is very smooth, with at least 2000 sources per square degree needed, and that the XRB is isotropic to better than a few percent in the 2–10 keV band. Cross-correlation analyses of the *HEAO 1* A-2 fluctuation data with galaxy catalogs (Jahoda et al. 1991; Lahav et al. 1993) show that only

~30% of the XRB intensity is due to a nonevolving population of X-ray sources correlated with present epoch ($z \lesssim 0.2$) galaxies (note that a population of heavily obscured galaxies would not contribute to that result). These constraints can be satisfied in the scenario investigated in this *Letter*, where the bulk of the XRB at 2–10 keV is supplied by a population of partially covered low-luminosity active galaxies at $z \gtrsim 3$. The unified Seyfert scheme of Antonucci & Miller (1985) predicts the existence of heavily obscured X-ray sources, and provides the physical motivation of our model. The dominant contributors to the observed XRB at $\gtrsim 3$ keV are self-absorbed Sey 2 galaxies, which have inverted spectra ($\alpha < 0$) for (rest-frame) energies less than 30 keV. These type 2 objects do not contribute to the *ROSAT* source counts or indeed to any of the present X-ray source counts to any significant amount. We also require that such objects are numerous to beyond $z \sim 2$. The observed steepening of the XRB intensity beyond 30 keV is due to a break or exponential cutoff in the primary X-ray photon distribution of the individual sources. Such a feature is indeed suggested by the observed spectra of Sey 1 galaxies obtained by OSSE. A population of weakly evolving, partially covered sources could, with some fine tuning of the optical depth of the blocking torus and temperature of the incident spectrum, fit the XRB quite well. While the required narrow range of kT -values might be explained by e^\pm pair production feedbacks in a thermal plasma (Svensson 1984; Zdziarski

1985), we do not know yet of any physical mechanism yielding a characteristic depth $\tau_T \sim 2$ –4. On the other hand, the ratio between the absorbed and the direct spectral component required by the fit is in agreement with estimates of the Sey 2 to Sey 1 number ratio derived from optical studies (e.g., Osterbrock & Shaw 1988). Analogously to the reflection scenario, the obscuration model is very inefficient in producing the XRB. Depending on the dimensions of the absorbing torus, its distance from the central photon source, and dust content, most of the power produced by the active nucleus will be re-emitted as thermal radiation at UV, optical or IR frequencies. If dust is present then the objects may be identified as faint *IRAS* (or *IRAS* band) galaxies.

Whatever the precise origin of the XRB, our work (and other work on reflection models) has shown that it is most plausibly explained by sources in which most of the emitted X-ray power is reprocessed in Thomson thick surrounding cold material. Since the XRB consists at least of the total escaping X-ray power from all AGNs, this conclusion emphasizes that *most* of the power of AGNs initially emitted at X-ray wavelengths is reprocessed.

It is a pleasure to thank R. Burg, J. Krolik, and A. Zdziarski for discussions and comments, and P. Zycki for kindly providing us with a compilation of the XRB data.

REFERENCES

- Antonucci, R. R. J., & Miller, J. S. 1985, *ApJ*, 297, 621
 Awaki, H. 1991, Ph.D. thesis, Nagoya Univ.
 Boyle, B. J. 1991, in Proc. Texas/ESO CERN Symp. Relativistic Astrophysics, Cosmology, and Fundamental Physics, ed. J. Barrow, L. Mestel, & P. Thomas (New York: NY Acad. Sci.), 24
 Cameron, R. A., et al. 1993, in Proc. Compton Symp. (St. Louis), ed. N. Gehrels, in press
 Della Ceca, R., Maccacaro, T., Gioia, I. M., Wolter, A., & Stocke, J. T. 1992, *ApJ*, 389, 491
 Fabian, A. C., & Barcons, X. 1992, *ARA&A*, 30, 429
 Fabian, A. C., George, I. M., Miyoshi, S., & Rees, M. J. 1990, *MNRAS*, 242, 14P
 Giacconi, R., Gursky, H., Paolini, F., & Rossi, B. 1962, *Phys. Rev. Lett.*, 9, 439
 Giacconi, R., & Zamorani, G. 1987, *ApJ*, 313, 20
 Grindlay, J. E., & Luke, M. 1990, in IAU Colloq. 115, High-Resolution X-Ray Spectroscopy of Cosmic Plasma, ed. P. Gorenstein & M. Zombeck (Dordrecht: Kluwer), 276
 Hasinger, G. 1992, in *The X-Ray Background*, ed. X. Barcons & A. C. Fabian (Cambridge: Cambridge Univ. Press), 229
 Hasinger, G., Schmidt, M., & Trumper, J. 1991, *A&A*, 246, L2
 Jahoda, K., Lahav, O., Mushotzky, R. F., & Boldt, E. A. 1991, *ApJ*, 378, L37
 Jourdain, E., et al. 1992, *A&A*, 256, L38
 Koyama, K. 1992, X-Ray Emission from Active Galactic Nuclei and the Cosmic X-Ray Background (MPE Rep. 235)
 Koyama, K., Inoue, H., Tanaka, Y., Awaki, H., Takano, S., Ohashi, T., & Matsuoka, M. 1989, *PASJ*, 41, 731
 Krolik, J. H., & Begelman, M. C. 1988, *ApJ*, 329, 702
 Lahav, O., et al. 1993, preprint
 Lightman, A. P., & White, T. R. 1988, *ApJ*, 335, 57
 Maisack, M., et al. 1993, in Proc. Compton Symp. (St. Louis), ed. N. Gehrels, in press
 Matsuoka, M., Piro, L., Yamauchi, M., & Murakami, T. 1990, *ApJ*, 361, 440
 Morisawa, K., Matsuoka, M., Takahara, F., & Piro, L. 1990, *A&A*, 236, 299
 Morrison, R., & McCammon, D. 1983, *ApJ*, 270, 119
 Mulchaey, J. S., Mushotzky, R. F., & Weaver, K. A. 1992, *ApJ*, 390, L69
 Osterbrock, D. E., & Shaw, R. A. 1988, *ApJ*, 327, 89
 Piccinotti, G., Mushotzky, R. F., Boldt, E. A., Holt, S. S., Marshall, F. E., Serlemitsos, P. J., & Shafer, R. A. 1982, *ApJ*, 253, 485
 Pounds, K. A., Nandra, K., Stewart, G. C., George, I. M., & Fabian, A. C. 1990, *Nature*, 344, 132
 Pozdnyakov, L. A., Sobol', I. M., & Sunyaev, R. A. 1983, *Ap&SS*, 2, 189
 Rogers, R. D., & Field, G. B. 1991, *ApJ*, 370, L57
 Rybicki, G. B., & Lightman, A. P. 1979, *Radiative Processes in Astrophysics* (New York: Wiley)
 Setti, G., & Woltjer, L. 1989, *A&A*, 224, L21
 Shanks, T., Georgantopoulos, I., Stewart, G. C., Pounds, K. A., Boyle, B. J., & Griffiths, R. E. 1991, *Nature*, 353, 315
 Sunyaev, R. A., & Titarchuk, L. G. 1980, *A&A*, 86, 121
 Svensson, R. 1984, *MNRAS*, 209, 175
 Terasawa, N. 1991, *ApJ*, 378, L11
 Wu, X., Hamilton, T., Helfand, D. J., & Wang, Q. 1990, *ApJ*, 379, 564
 Zdziarski, A. A. 1985, *ApJ*, 289, 514
 Zdziarski, A. A., Zycki, P. T., Svensson, R., & Boldt, E. 1993, *ApJ*, 405, 125